AD-A058 451 AMPEX CORP REDWOOD CITY CA ADVANCED TECHNOLOGY DIV F/G 14/3
FOIL BEARING INVESTIGATION. A FOIL BEARING MODEL FOR HIGH SPEED--ETC(U)
AUG 78 A ESHEL, T G KENNEDY N00014-77-C-0021
UNCLASSIFIED RR-78-10 NL

END
DATE FILMED
11-78
DDC

AMPEX

LEVEL III

12

B.S.

FOIL BEARING INVESTIGATION

A Foil Bearing Model for High Speed Rotating Magnetic Heads

Prepared Under: Contract No. N00014-77-C-0021
Task NR 062-297
Office of Naval Research

Administered by: Scientific Officer
Mathematical and Information Sciences Division
Office of Naval Research
800 North Quincy Street
Mr. Stanley W. Doroff, Code 438
Arlington, Virginia 22217

Prepared by: A. Eshel
A. Eshel
Member of the Research Staff
T. G. Kennedy
T. G. Kennedy
Research Associate

Approved by: F. K. Orcutt
F. K. Orcutt
Manager, Mechanics Section

M. Wildmann,
Manager, Research Department

RR78-10

Unclassified

SECURITY CLASSIFICATION OF THIS PAGE (When Data Entered)

REPORT DOCUMENTATION PAGE	READ INSTRUCTIONS BEFORE COMPLETING FORM
(11) 1. REPORT NUMBER RR-78-10	2. GOVT ACCESSION NO. AD-A045208	3. RECIPIENT'S CATALOG NUMBER
(9) 4. TITLE (and Subtitle) FOIL BEARING INVESTIGATION, A Foil Bearing Model for High Speed Rotating Magnetic Heads	5. TYPE OF REPORT & PERIOD COVERED (9) Technical Rept.,
	6. PERFORMING ORG. REPORT NUMBER
7. AUTHOR(s) (10) A. Eshel and T. G. Kennedy	8. CONTRACT OR GRANT NUMBER(s) (15) N00014-77-C-0021
9. PERFORMING ORGANIZATION NAME AND ADDRESS Ampex Corporation, Advanced Technology Division 401 Broadway Redwood City, CA 94063	10. PROGRAM ELEMENT, PROJECT, TASK AREA & WORK UNIT NUMBERS NR 062-297
11. CONTROLLING OFFICE NAME AND ADDRESS Office of Naval Research, Dept. of the Navy 800 N. Quincy Street (Code 613B: DRVM) Arlington, VA 22217	(11) 12. REPORT DATE 29 August 1978
	13. NUMBER OF PAGES 23
14. MONITORING AGENCY NAME & ADDRESS(if different from Controlling Office)	15. SECURITY CLASS. (of this report) Unclassified
	15a. DECLASSIFICATION/DOWNGRADING SCHEDULE
16. DISTRIBUTION STATEMENT (of this Report) Approved for public release; distribution unlimited. (12) 24 p.	
17. DISTRIBUTION STATEMENT (of the abstract entered in Block 20, if different from Report)	
18. SUPPLEMENTARY NOTES flow are presented. Foil Bearings Self Acting Foil Bearings Helical Scan Tape Recorders Rotating Magnetic Heads Moving Loads on Beams	
19. KEY WORDS (Continue on reverse side if necessary and identify by block number)	
20. ABSTRACT (Continue on reverse side if necessary and identify by block number) A quasi one-dimensional foil bearing model for high speed rotating magnetic heads has been formulated. Side flow is "smeared" as a leakage factor. Steady state foil inertia effects are included. The effects of head protrusion side leakage factor as well as speed parameter are discussed. Of particular interest is the effect of rotational speed in relation to the propagation speed of transverse waves in the foil.	

403 899 78 08 31 021

DD FORM 1 JAN 73 1473 EDITION OF 1 NOV 65 IS OBSOLETE Unclassified

SECURITY CLASSIFICATION OF THIS PAGE (When Data Entered)

NOMENCLATURE

a	characteristic dimension in side flow direction
D	bending stiffness of foil
F	dimensionless deviation of foil contour $W_f - 1$
h	local fluid film thickness
h^*	asymptotic film thickness away from the head
H	dimensionless film thickness h/h^*
p	local pressure under foil
p_a	ambient pressure
p_∞	pressure under foil in vicinity of head
r_o	drum radius
t	time
T_f	foil tension per unit width
U_f	foil velocity (in +x direction)
U_r	drum velocity
W	dimensionless foil contour w/h^*
w_f	foil contour (function of x and t)
w_{max}	head protrusion
w_r	bump contour (function of x)
x	circumferential position along drum
β	side flow parameter, proportional to $(\delta/a)^{**2}$
δ	head width at base
ϵ	speed parameter (Eq. 12)
μ	air viscosity
σ	foil mass per unit area
τ	dimensionless time (Eq. 10)
ξ	dimensionless circumferential position x/δ

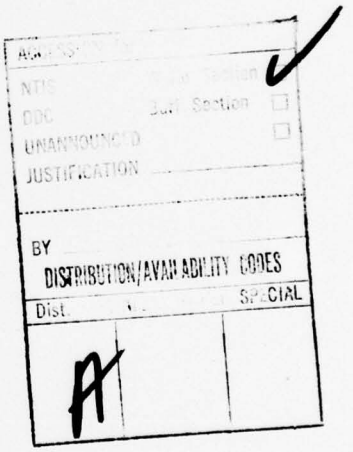

INTRODUCTION

High density tape recorders in computer and instrumentation applications utilize a geometry schematically shown in Figure 1. A drum in which a magnetic head is imbedded, rotates at a high speed. The tape is wrapped around the drum and is floated over it with a fairly thick clearance (order of 25 microns). Due to the rotational speed, the tape tends to float also at a considerable separation from the head. It is desired, however, that the head interface the tape at a close proximity (a fraction of a micron). This task is achievable by especially contouring and grooving the head to promote reduction of the hydrodynamic film thickness to the desired level. The effects of side flow are thus of significance. Due to the high speed of drum rotation, the effects of foil inertia are also of importance. In fact, one may think of the head as forming a concentrated travelling load.

The objective of the present report is to approximate on a quasi one-dimensional basis as many effects as possible of the configuration described in Figures 1-3. Specifically, the effects of head contour and protrusion, side flow (represented by a "smeared" leakage factor), foil inertia, tension and speed will be discussed. Results as to the effect of the various parameters will be reported.

A selection from the relevant literature is mentioned below. The elastic effects of travelling concentrated disturbances in plates or foils have been studied by Kenney [1], Reismann [2], Bogy, Greenberg and Talke [3], and Adams and Bogy [4]. Langlois [5] studied a quasi two dimensional membrane model with lubrication effects included. Dais and Barnum [6] looked into the effect of a rotating drum with a flat. Greenberg [7] investigated the interface of a magnetic head with a flexible disk. Eshel examined the effect of a travelling external pressure feed hole [8]. Stahl, White and Deckert [9] published work on dynamic effects, taking foil inertia into consideration. In the experimental area, the main available work is by Albrecht, Laenen and Chua Lin [10] who reported measurements of foil contours in response to travelling bumps.

ANALYSIS

Figure 1 describes schematically the model being studied. A drum of radius r_o, with a bump of a specified contour $w_r(x)$ rotates with a surface velocity U_r. Here, x is a circumferential coordinate fixed in the drum. The foil wraps the drum, and its contour $w_f(x,t)$ as well as the foil to drum separation $h(x,t)$, are the subject of the investigation. An essentially planar model is being studied here. It is assumed, however, that part of the circumferential flow is removed by side flow into appropriate grooves. An approximate mathematical model for the side flow is hypothesized later. The force balance across the foil is:

$$p-\left(p_a+\frac{T_f-\sigma U_f^2}{r_o}\right)-D\frac{\partial^4 w_f}{\partial x^4} \qquad (1)$$

$$=\sigma\left(\frac{\partial^2 w_f}{\partial t^2}+2\left(U_f-U_r\right)\frac{\partial^2 w_f}{\partial x\,\partial t}-\frac{T_f-\sigma\left(U_f-U_r\right)^2}{\sigma}\frac{\partial^2 w_f}{\partial x^2}\right)$$

The one-dimensional Reynolds equation in these coordinates with a local leakage correction factor included is:

$$\frac{\partial}{\partial x}\left(h^3 p\frac{\partial p}{\partial x}-6\mu\left(U_f-U_r\right)ph\right)-\left(\begin{matrix}\text{SIDE}\\ \text{LEAKAGE}\end{matrix}\right)=12\mu\frac{\partial ph}{\partial t}$$

where

$$\text{SIDE LEAKAGE} \equiv \frac{\partial}{\partial y}\left(h^3 p\frac{\partial p}{\partial y}\right) \qquad (3)$$

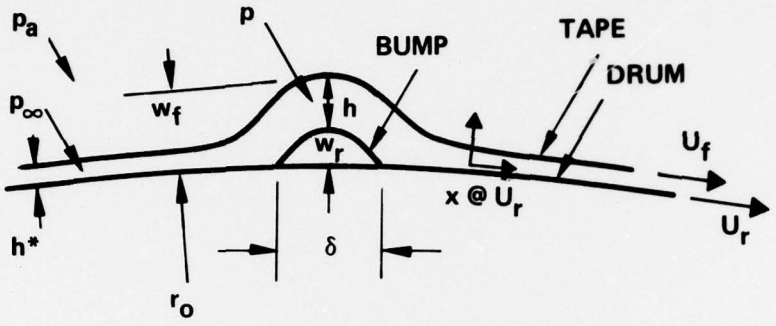

Figure 1 Schematic View of a Drum, Bump and Foil

TYPICAL SIDE FLOW CONTROLLING DIMENSION

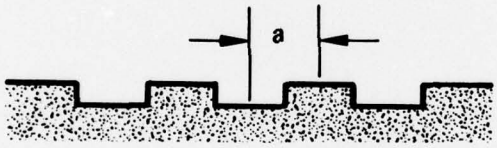

Figure 2 View of Lateral Contour of a Grooved Bump

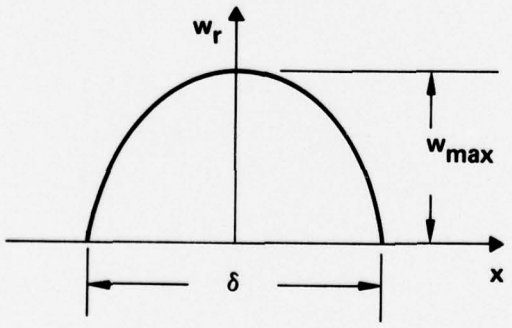

Figure 3 Bump Dimensions

In the problem studied here, the pressure under the foil and the film thickness are assumed to reach some constant values p_∞ and h^*, respectively, sufficiently far away from the bump. According to (1), then

$$p_\infty - p_a = \frac{T_f - \sigma U_f^2}{r_0} \tag{4}$$

Neglecting foil stiffness, Eq. (1) may be rewritten as

$$p - p_\infty = \sigma \frac{\partial^2 w_f}{\partial t^2} + 2\sigma (U_f - U_r) \frac{\partial^2 w_r}{\partial x \partial t} - \left[T_f - \sigma (U_f - U_r)^2 \right] \frac{\partial^2 w_f}{\partial x^2} \tag{5}$$

In the incompressible case, a simple model for the leakage factor is

$$\text{(SIDE LEAKAGE)} \qquad \sim (p - p_\infty) \frac{h^3}{a^2} \tag{6}$$

where "h" is a characteristic film thickness and "a" is a typical side flow dimension (Fig. 2).

The differential equations (2), (5) must be supplemented by the relation

$$w_f = w_r + h \tag{7}$$

Assuming that the bump shape may be approximated by a parabola, w_r is given by

$$w_f = \begin{cases} w_{max} \left(1 - \left(\frac{x}{\delta/2} \right)^2 \right) ; & \frac{\delta}{2} > |x| \\ 0 ; & \frac{\delta}{2} < |x| \end{cases} \tag{8}$$

where w_{max} is the bump protrusion and δ its base width.

The boundary conditions for Eqs. (2), (5) – (8) are:

$$\begin{array}{lll} x \to -\infty & h \to h^* & p \to p_\infty \\ x \to \infty & \dfrac{dh}{dx} \to 0 & p \to p_\infty \end{array} \qquad (9)$$

It is to be noted that if the level of h* is prescribed at $-\infty$, one is not free to specify it at $x \to \infty$ (due to the side flow).

NORMALIZATION

The following normalizations will be used

$$\left.\begin{array}{llll} H = \dfrac{h}{h^*} & W_f = \dfrac{w_f}{h^*} & W_r = \dfrac{w_r}{h^*} & F = W_f - 1 \\ \xi = \dfrac{x}{\delta} & \tau = \dfrac{T_f - \sigma (U_f - U_r)^2}{12 \mu \delta^4} h^{*3} t & & \end{array}\right\} \qquad (10)$$

If we neglect time dependent inertia effects as seen from the moving coordinate ($\frac{\partial}{\partial t} \equiv 0$ in Eqn. (5)), and assume incompressible flow, we find using the above

$$\beta H^3 \frac{\partial^2 F}{\partial \xi^2} - \frac{\partial}{\partial \xi}\left(H^3 \frac{\partial^3 F}{\partial \xi^3}\right) - \epsilon \frac{\partial F}{\partial \xi} = -\epsilon \frac{\partial W_r}{\partial \xi} + \frac{\partial F}{\partial \tau} \qquad (11)$$

where β is a proportionality leakage parameter

$$\beta \sim \frac{\delta^2}{a^2} \qquad (12)$$

and ϵ, the speed parameter

$$\epsilon = \frac{6\mu (U_f - U_r)}{T_f - \sigma (U_f - U_r)^2} \cdot \frac{\delta^3}{h^{*3}} \qquad (13)$$

$$H = 1 + F - W_r \qquad (14)$$

The bump shape is

$$W_r = \begin{cases} W_{max}(1-4\xi^2) & 0.5 > |\xi| \\ 0 & 0.5 < |\xi| \end{cases} \qquad (15)$$

The boundary conditions for steady state are:

$$\begin{array}{lll} \xi \to -\infty & F \to 0 & F'' \to 0 \\ \xi \to \infty & F' \to 0 & F'' \to 0 \end{array} \qquad (16)$$

The steady state solution of the problem may, thus, be expressed as

$$F = F(\xi; \beta, \epsilon, W_{max})$$

RESULTS AND DISCUSSION

Computer programs have been developed to study the model described above. In this report a limited range of results of interest are presented. Further results will be published in future reports. The present results are based on the following assumptions.

1. Planar flow
2. The local side leakage is a constant times ($p-p_\infty$), i.e., it is assumed that $H \equiv 1$ in the side leakage term of Eqn. (11).
3. Fluid inertia effects are neglected.
4. Only the steady state foil inertia effects (in terms of the moving coordinate) are included.
5. Foil stiffness is neglected.

6. Fluid compressibility is neglected.

7. The head shape is a parabola of specified height, intersecting the drum with a specified width δ.

Two sequences of Figures represent the main results. Figures (4a)-(4c) show steady state foil contours in relation to head shape under various conditions. Figures (6)-(8) summarize the effects of various parameters on the minimum head to tape separations.

In Figure (4a), the effect of ϵ is studied. For concreteness, one may think of ϵ as a speed parameter. As the speed increases, the film thickness in the rear of the head grows, whereas in front of the head, the film thickness decreases due to the "inertial impact" of the tape, or, putting it differently, due to the tape "getting in the way" of the moving head.

It is to be noted, however, that as the value of U_f-U_r goes through the propagation speed of transverse waves in the foil $\sqrt{\frac{T_f}{\sigma}}$, (referred to loosely as "sonic speed"), the sign of ϵ changes (Figure 5). As long as the head shape is symmetrical, the solution for a given $+\epsilon$ is a reflection about the head axis of the solution for $-\epsilon$ (see Fig (4a) for $\epsilon = \pm 100$). This fact clearly hints to useful variations achievable by non-symmetric heads.

In Figures (4b) and 7, the effects of side leakage are demonstrated. By increasing β, the side leakage parameter, the film thickness in the rear of the bump is reduced. Thus, side flow provides a means for controlling head to tape separation in recording. Finally, the effect of head protrusion over the drum is illustrated in Figs (4c) and is summarized in Figure 8. This factor is, again, important in achieving the desired flying characteristics on recording. It is perhaps worth mentioning that for sufficiently large β and w_{max}, head to tape separation may be reduced until contact is established.

One may note that in the "subsonic" case, waves appear in front of the head, whereas in the supersonic case they appear in the rear. Figure 9 shows the wavelength of the tape contour as a function of β and ϵ. It is interesting to remark that for each value of β, there is a value of ϵ below which no waves exist.

In conclusion, this work has resulted in the development of computer programs modelling head to tape interface in helical recorders. The effects of speed, tension, side flow and head protrusion may be studied for different head geometries and for optimization purposes.

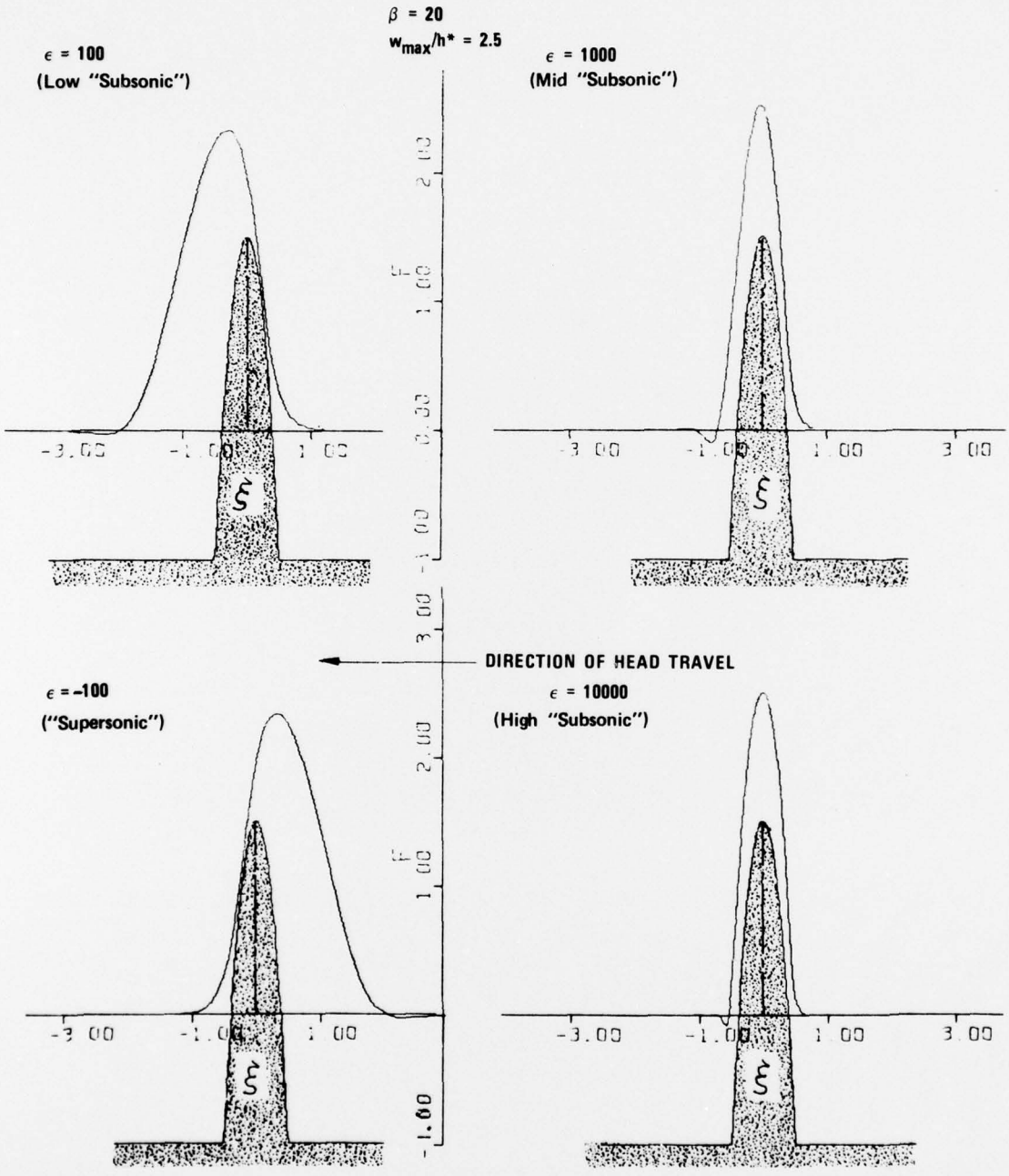

Figure (4a) Steady State Tape Contour Over a Travelling Head: Effect of Speed Parameter ϵ

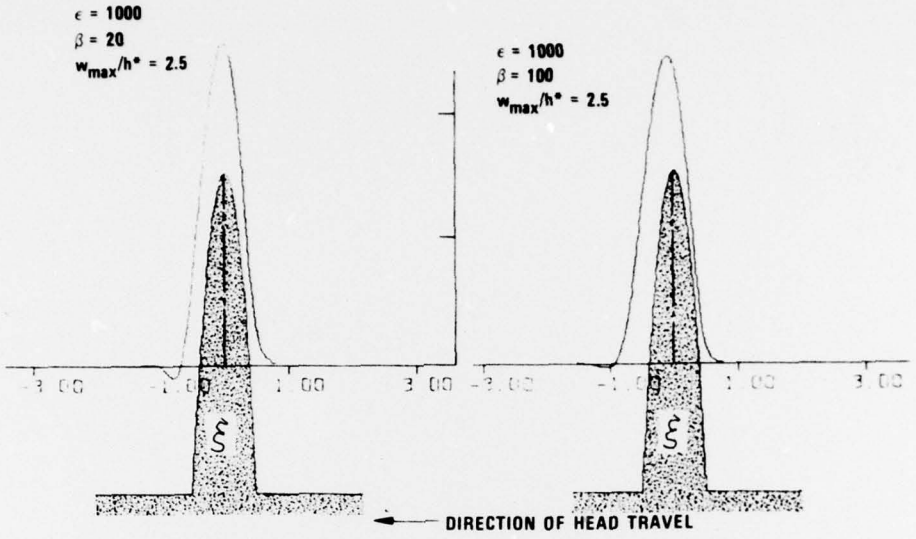

Figure (4b) Steady State Tape Contour Over a Travelling Head: Effect of Side Leakage Parameter β

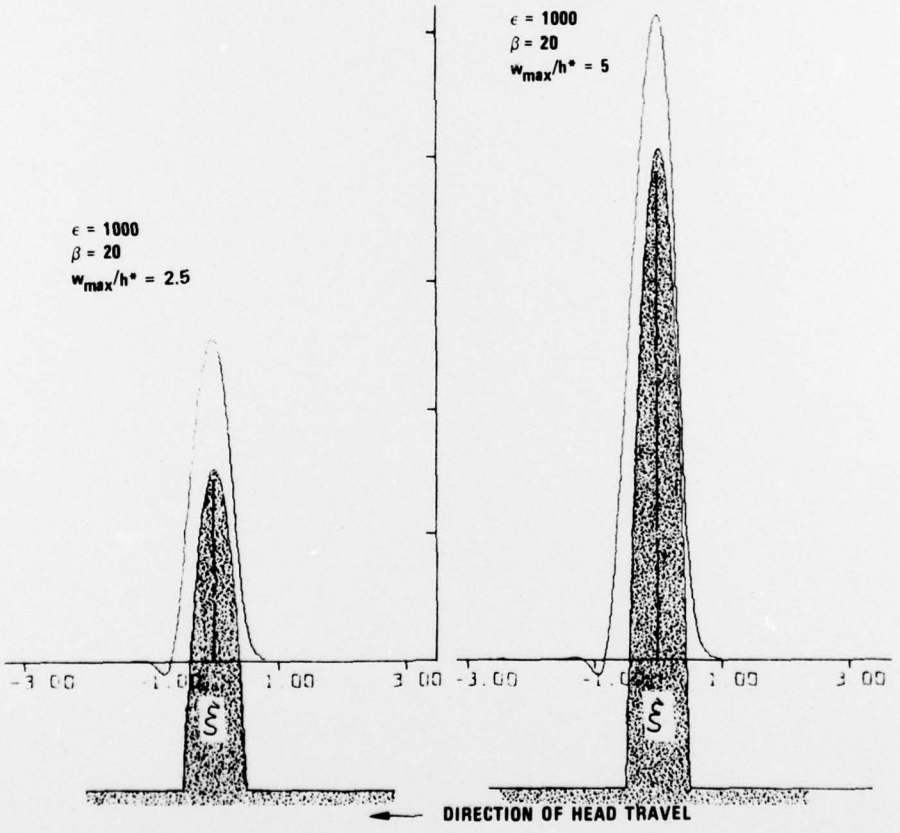

Figure (4c) Steady State Tape Contour Over a Travelling Head: Effect of Head Protrusion

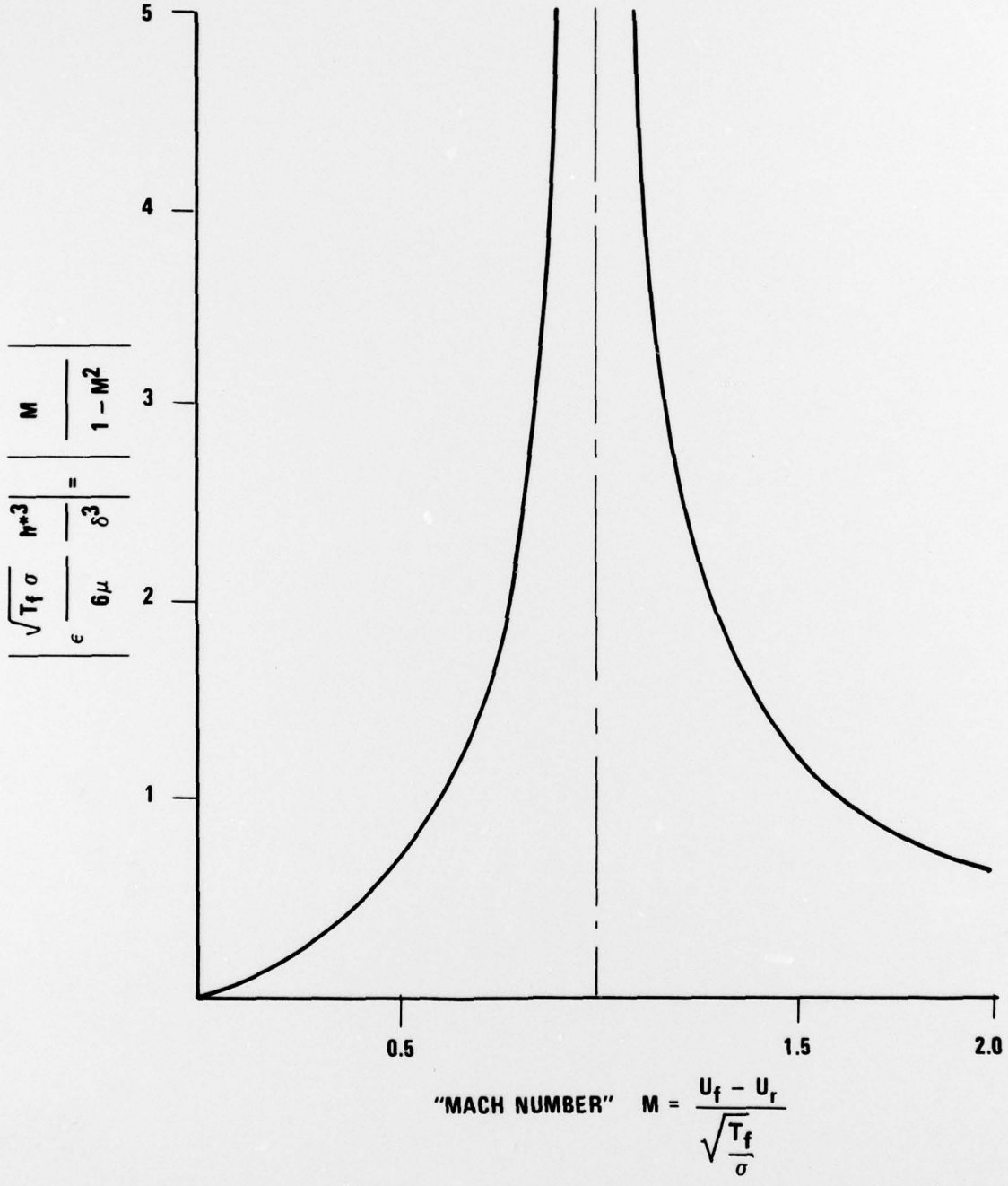

Figure 5 Variation of Speed Parameter Magnitude with "Mach Number"

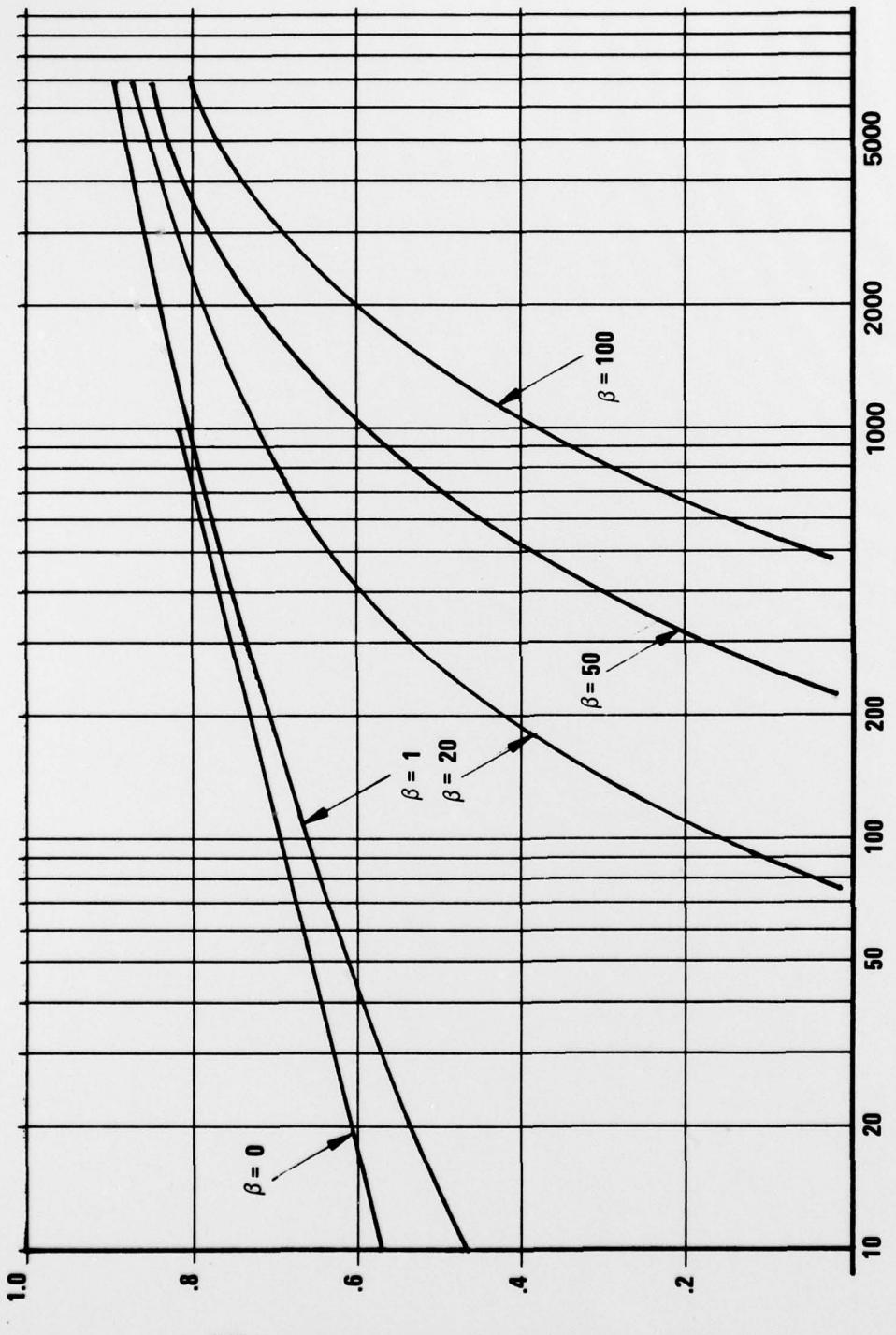

Figure 6 Minimum Film Thickness vs Speed Parameter

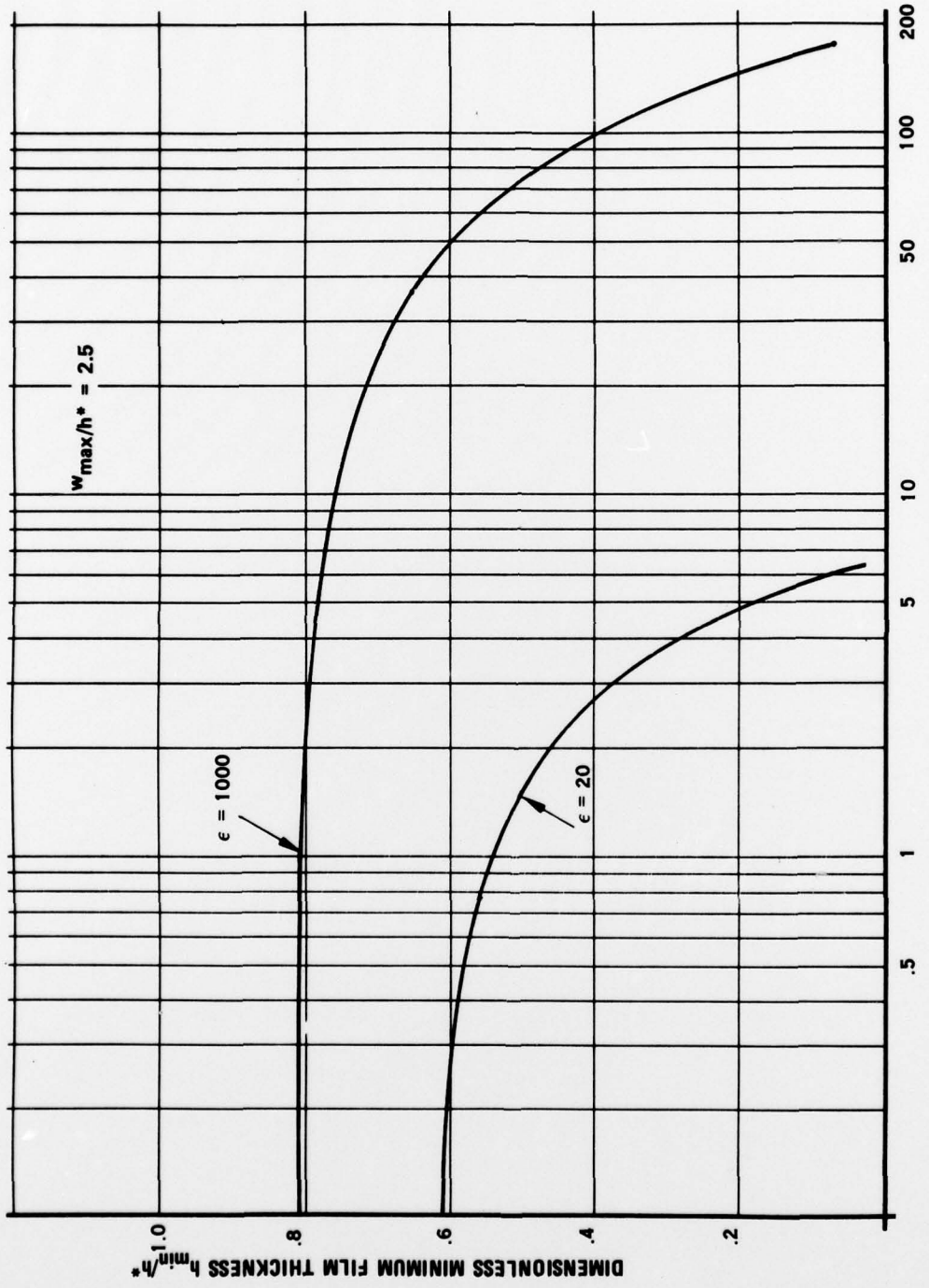

Figure 7 Minimum Film Thickness vs Side Leakage

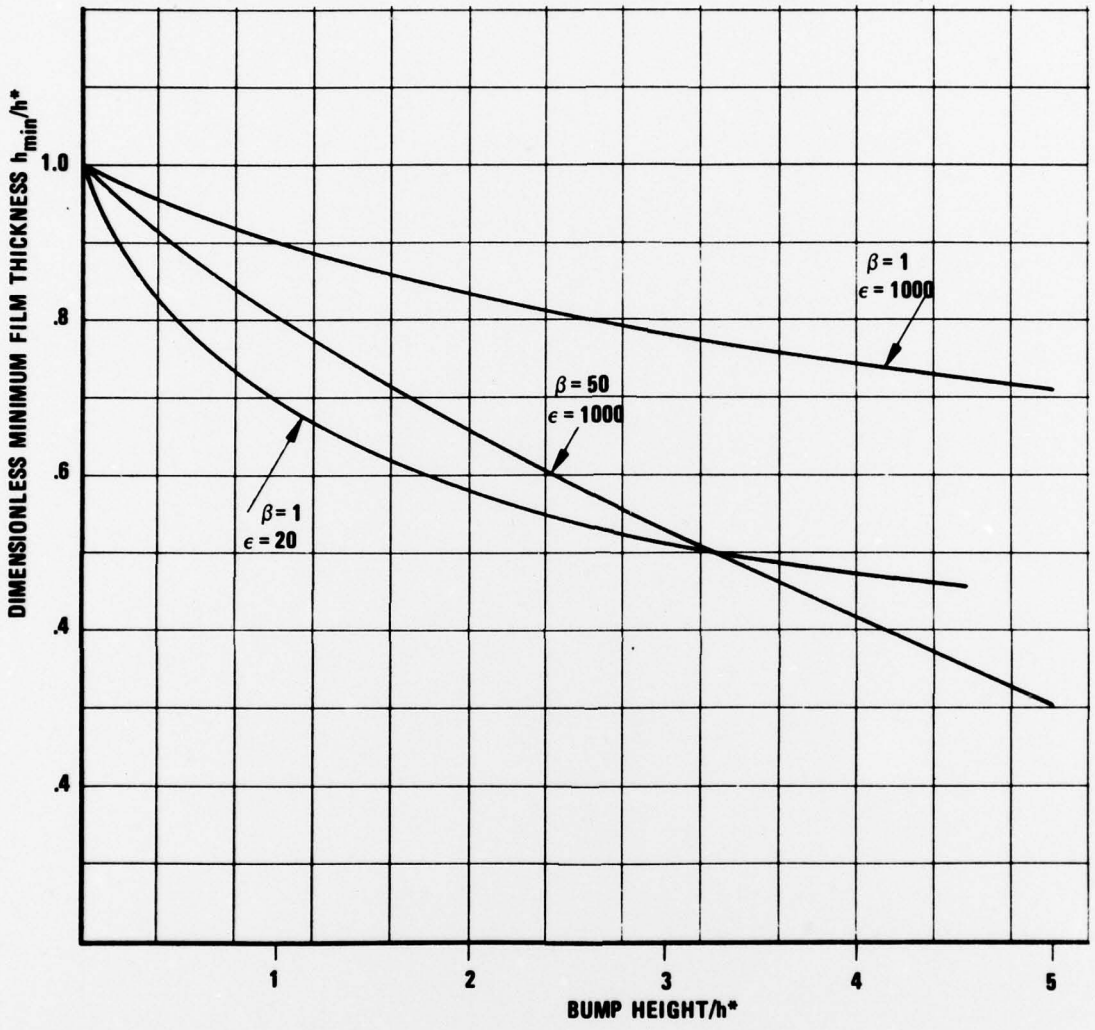

Figure 8 Minimum Film Thickness vs Bump Height

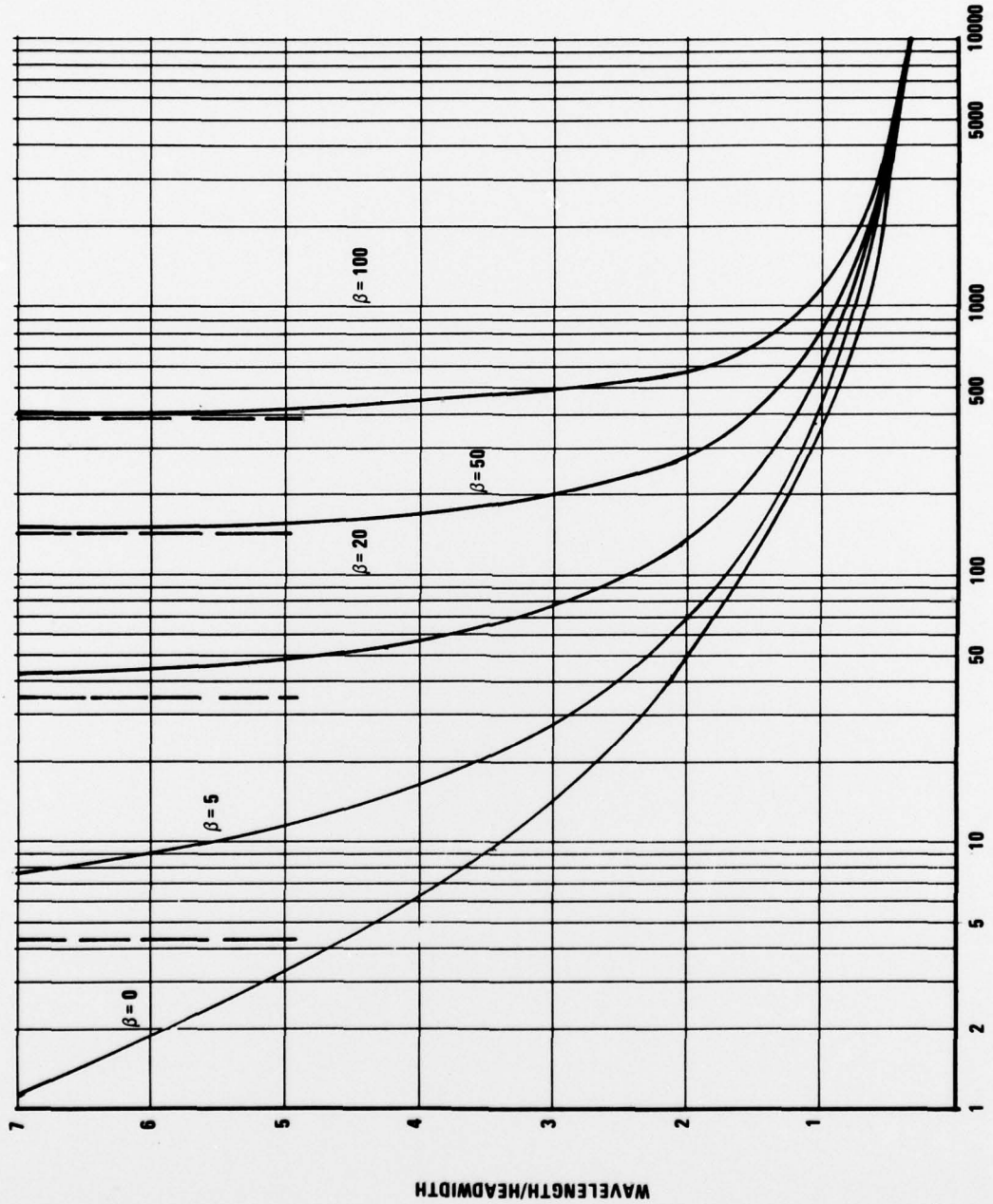

Figure 9 Wavelength of Tape Contour vs Speed Parameter

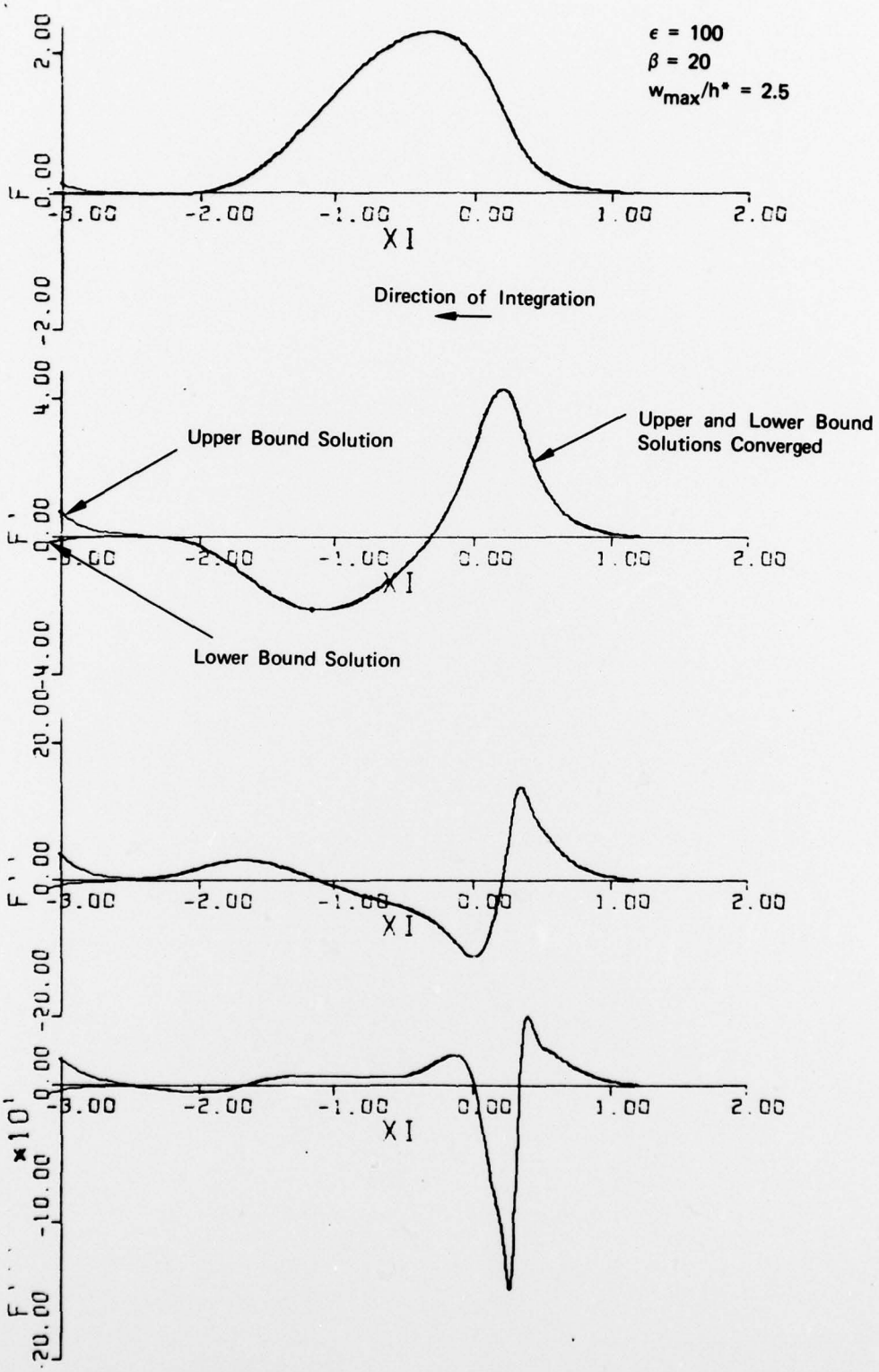

Figure 10 Typical O.D.E. Solution. Upper and Lower Bound on the Function F and its Derivatives for Positive ϵ

REFERENCES

1. T. J. Kenney, Jr., "Steady State Vibrations of Beam on Elastic Foundation for Moving Load", Trans. ASME, J. App. Mech, 1954, pp 359-364.

2. H. Reisman, "Dynamic Response of an Elastic Plate Strip to a Moving Line Load", AIAA J. 1964, pp 354-360.

3. D. B. Bogy, H. T. Greenberg and F. E. Talke, "Steady State Solution for Circumferentially Moving Loads on Cylindrical Shells", IBM J. Res. Develop. 1974, pp 395-400.

4. G. G. Adams and D. B. Bogy, "Steady Solutions for Moving Loads on Elastic Foundation with One Sided Constraints", Trans. ASME, J. App. Mech. 1975, pp 800-804.

5. W. E. Langlois, "Finite Width Foil Bearing with Light Loading", Trans. ASME, J. App. Mech. 1975, pp 274-278.

6. J. L. Dais and T. B. Barnum, "The Geometrically Irregular Foil Bearing", Trans. ASME J. Lub. Tech. 1974, pp 224-227.

7. H. J. Greenberg, "Flexible Disk - Read/Write Head Interface", Presented at IEEE Proc. Intermag. Conf. 1978, Italy.

8. A. Eshel, "Transient Analysis of a Planar Hybrid Foil Bearing", Trans. ASME J. Lub. Tech. 1974, pp 433-435.

9. K. J. Stahl, J. W. White and K. L. Deckert, "Dynamic Response of Self Acting Foil Bearings", IBM J. Res. Develop. 1974, pp 513-520.

10. D. M. Albrecht, E. G. Laenenand and Chua Lin, "Experiments on Dynamic Response of a Flexible Strip to Moving Loads, " IBM J. Res. Develop. 1977, pp 379-383.

11. A. Eshel and H. G. Elrod Jr. "The Theory of the Infinitely Wide, Perfectly Flexible, Self Acting Foil Bearing", Trans. ASME J. Lub. Tech. 1965, pp 831-836.

12. A. Eshel, Numerical Solution of the Planar Hydrostatic Foil Bearing", to be presented ASME-ASLE lubrication conference, Minneapolis, Minnesota, 1978.

13. D. B. Reed, "On Numerical Solution of the Three Dimensional Vorticity Equation", Trans. ASME, J. of Fluid Engineering, 1976 pp 770-771.

14. A. Sereny and V. Castelli, "Numerical Solution of Reynolds Equation with Slip Boundary Conditions for Cases of Large Bearing Numbers", to be Published Trans. ASME, J. of Lub. Tech.

APPENDIX – NUMERICAL TECHNIQUES

This appendix describes two numerical techniques utilized for obtaining the solutions presented.

(a) Steady State Asymptotic O.D.E.

If one limits interest to the asymptotic steady state behavior, the time dependent term in Eqn. (1) may be dropped. With the side leakage term approximated as $\beta \frac{d^2F}{d\xi^2}$, the equation may be integrated once to

$$\frac{d^3F}{d\xi^3} = \frac{\beta \frac{dF}{d\xi} - \epsilon F + \epsilon W_r}{(1+F-W_r)^3}$$

To satisfy the boundary conditions at $\pm\infty$, a linearized from of the equation may be utilized, i.e.,

$$\frac{d^3F}{d\xi^3} - \beta \frac{dF}{d\xi} + \epsilon F = 0$$

For $\epsilon > 0$, the solution of this equation is used to start numerical integration in the $-\xi$ direction, after eliminating the exponential components of the solution that do not satisfy the boundary conditions. The method of solution is described in greater detail in [11], where it is applied to a different problem. Different trials

generate upper and lower bounds for the solution. Once convergence is achieved, the upper and lower bound solutions deviate from one another only for large values as shown in Figure 10. For $\epsilon<0$, the solution is a reflection about $\xi=0$.

The main advantage of this solution method is the variable grid size which is related to the local truncation error, leading to high accuracy. Its disadvantage is the sensitivity of the solution to low film thicknesses due to the appearance of H^3 in the denominator.

(b) Time Dependent Solution

The time history of the foil contour may be numerically solved from Eqn. (11). As an alternative to the technique described above, the steady state solution may be found as the asymptotic limit of the time history. This approach is particularly attractive since we have at our disposal a precompiler [12] which permits the generation of such a solution with relative ease. It should be emphasized, however, that in the derivation of Eqn. (11), the time dependent terms of Eqn. (5) have been neglected. Furthermore, τ (Eqn. 10) contains the factor which "reverses" time for "supersonic" speeds. Therefore, Eqn. (11) constitutes a true physical representation of unsteady phenomena only for low "subsonic" speeds. For higher speeds and, especially for "supersonic" speeds Eqn. (11) should be interpreted merely as a mathematical device for obtaining steady state solutions.

The present project helped to focus on some desired improvements in the precompiler.

1. A three dimensional plot program has been incorporated into the precompiler which helps assess how far the behavior has reached asymptotically. The result of the plot program is illustrated in Figure 11.

2. The method of discretization of the term

   $\frac{\partial}{\partial \xi}\left(H^3 \frac{\partial^3 F}{\partial \xi^3}\right)$ has significant effects on the results. If $\delta^n F$ denotes the central difference operator of order n, the discretization

$$\frac{\partial}{\partial \xi}\left(H^3 \frac{\partial^3 F}{\partial \xi^3}\right) \approx \delta'\left(H^3 \delta^3 F\right) \qquad \text{(A1)}$$

works well, whereas the discretization

$$\frac{\partial}{\partial \xi}\left(H^3 \frac{\partial^3 F}{\partial \xi^3}\right) = 3H^2 \frac{\partial H}{\partial \xi} \frac{\partial^3 F}{\partial \xi^3} + H^3 \frac{\partial^4 F}{\partial \xi^3} \qquad \text{(A2)}$$

$$\approx 3H^2 \delta H \delta^3 F + H^3 \delta^4 F$$

introduces mass conservation errors. A similar problem has been reported in [13, 14]. The capability of discretizing according to (A1) is being introduced into the precompiler.

3. Finally, the need for fine discretization in the fast varying regions of the problem vs coarse discretization in the slowly varying regions, is quite acute in the present problem. Efforts are underway to incorporate in the precompiler a variable grid size capability.

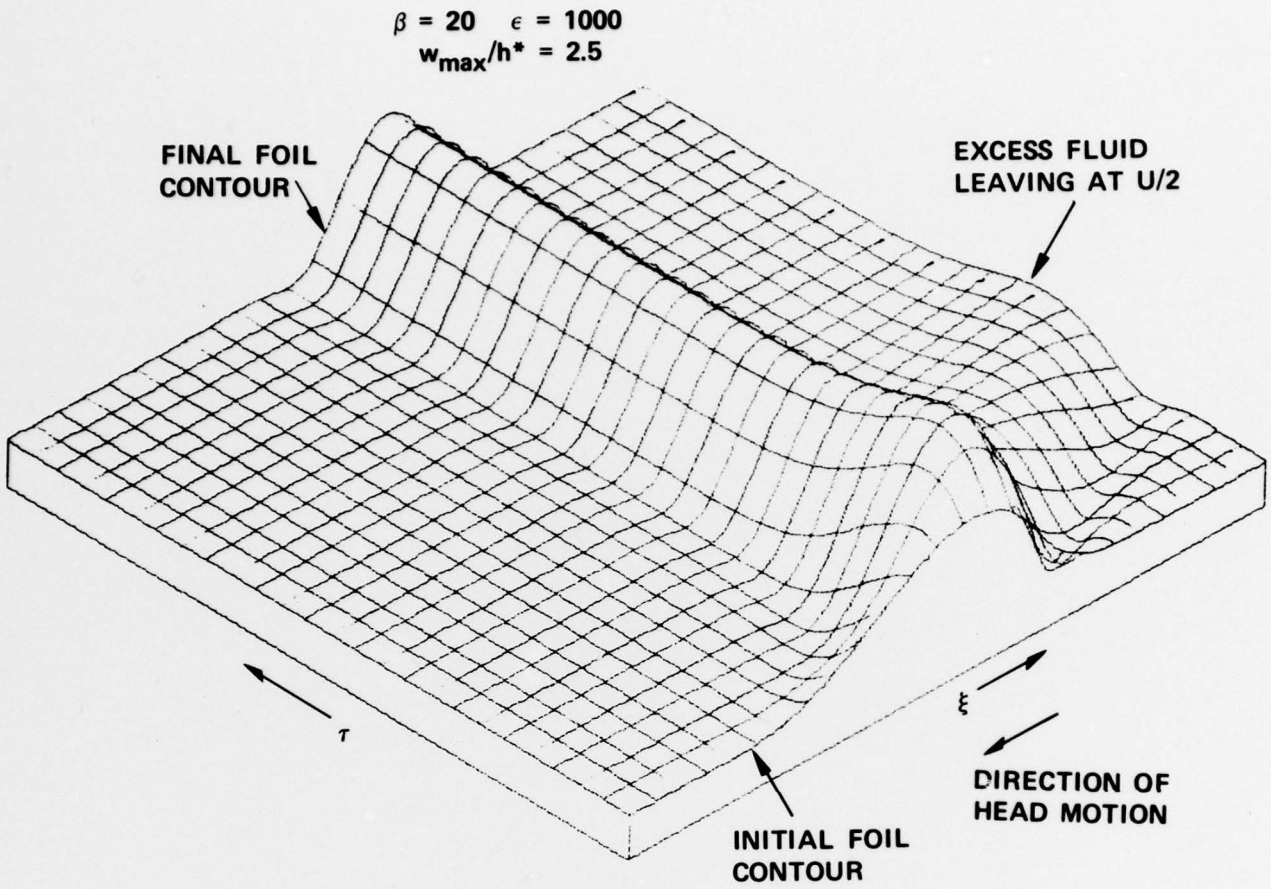

Figure 11 Development of Foil Contour From an Arbitrarily Prescribed Initial Condition, as Seen From a Reference Moving with the Head